Analysis of the Interaction of the Nucleotide Base with Myosin and the Effect on Substrate Efficacy

David Hyatt,[†] Roger Cooke,[‡] and Edward Pate[†*]
[†]Department of Mathematics, Washington State University, Pullman, Washington; and [‡]Department of Biophysics and Biochemistry, Cardiovascular Research Institute, University of California, San Francisco, California

ABSTRACT A wide variety of purine- and pyrimidine-based nucleotides can serve as a substrate for actomyosin mechanics, but with varying effectiveness. To understand the myosin-ATP interaction and in particular, the interactions with the base, we have used molecular dynamics simulations to model the interactions of myosin with ATP, CTP, UTP, aza-ATP, ITP, and GTP (in decreasing order of effectiveness as a substrate for the generation of motility) docked at the active site. The simulations with ATP, and x-ray structures, show a triad of conserved amino acids lining the nucleotide site that form a cyclical chain of nucleotide-protein hydrogen bonding interactions: ATP → Y135 → Y116 → N188 → ATP. Mechanical efficacy of a substrate correlates with its ability to maintain this coordination. Simulations modeling the active site of other myosin isoforms with different amino acids in the triad likewise imply that the amino acid composition at the nucleotide site could modulate function. The modeling has predictive power. In silico mutation experiments suggest mutations that would enhance GTP as a substrate for myosin while simultaneously making ATP a less effective substrate.

INTRODUCTION

Determining the mechanism by which the motor protein, myosin, produces biologically useful force and motion remains a fundamental, unresolved question in muscle physiology. The hydrolysis of ATP to ADP and inorganic orthophosphate provides chemical free energy driving the process. However, an atomic-level understanding of the force-generating interaction of the nucleotide with the motor protein remains elusive.

Myosin is a member of the G-protein superfamily of NTPases (1–3). The structural correlations between myosin and the G-proteins have led to considerable interest in interactions between the γ-phosphate moiety of the nucleotide and the conserved switch-1 and switch-2 motifs at the active site, and their implications for the generation of force. The original structural changes seen in the x-ray structures of the myosin motor domain with ADP·BeF_3 and ADP·Vi at the active site (4,5) motivated the current hypothesis linking conformational changes at the nucleotide site associated with hydrolysis to conformational changes associated with motility. The tetrahedral fluorine coordination in ADP·BeF_3 makes it an ATP analog. The trigonal, bipyramidal coordination of ADP·Vi makes it an analog of the planar oxygen coordination of the hydrolysis transition state intermediate. Conformational changes were observed in switch 2 adjacent to the γ-phosphate and in a long α-helix located C-terminus to switch 2 associated with the different conformations of the γ-phosphate moiety. These were accompanied by a rotation of the myosin structure adjacent to the neck. The magnitude of the rotation was compatible with generating the experimentally determined working step length of myosin (4, 6–10). Computational modeling has supported a coupling of movements of switch 2 to orientational changes in the neck region of myosin (11–16).

However, myosin is a promiscuous enzyme that can hydrolyze a large number of nucleotide triphosphate species in addition to ATP. Modifications of both the base and ribose are tolerated, albeit with varying mechanical efficacy (17–25). Most surprisingly, compounds termed ''nanalogs'' (a substituted phenyl ring in lieu of the base and an aminoethyl spacer substituting for the ribose) also support active contraction in muscle, but again with graded efficacy (26–28). Many of the nanalogs are hydrolyzed at rates comparable to ATP, but yield no force or sliding velocity (26,27). Thus the interactions at the γ-phosphate position of the substrate may be necessary for contraction, but they are clearly not sufficient. Indeed, the current view regarding conformational changes that drive motility via the interaction of the γ-phosphate of the substrate with the switch regions would not seem to preclude tripolyphosphate from serving as a substrate for contraction. However, tripolyphosphate is not a substrate for motility in skinned fibers (E. Pate, unpublished observations). Thus, the conversion of chemical energy to mechanical energy by myosin must be modulated by protein interactions at the γ-phosphate and with the remainder of the substrate as well.

X-ray structures of myosin have been solved only for adenine-based nucleotides and nanalogs at the nucleotide site (29). To understand the nucleotide-protein interactions that are crucial for function, we have used molecular dynamics (MD) simulations to probe the myosin·substrate interaction for a series of nucleotide triphosphate substrates of varying mechanical efficacy docked at the active site of the *Dictyostelium* myosin·BeF_3 x-ray structure (4).

Submitted April 17, 2009, and accepted for publication July 14, 2009.

*Correspondence: epate@wsu.edu

Editor: Christopher Lewis Berger.

© 2009 by the Biophysical Society

0006-3495/09/10/1952/9 $2.00

doi: 10.1016/j.bpj.2009.07.022

This allows us to suggest crucial interactions between the base-portion of the substrate and the protein, and additional intraprotein interactions at the active site that are essential for function. To be of use, any modeling analysis must be able to be predictive in the face of modifications at the active site. GTP is an extremely poor substrate for myosin (19,21, 22,24). Our MD simulations allow us to suggest mutations at the active site that would enhance its function as a substrate for the actomyosin system.

METHODS

The x-ray structure of *Dictyostelium* myosin·ADP·BeF_3 (Protein Data Bank (PDB) 1MMD) (4) was used as the starting point for simulations with a nucleotide at the active site. The BeF_3 moiety was converted to a γ-phosphate by editing the PDB file. The base was then modified as appropriate for the simulation. Structures are shown in Fig. S1 of the Supporting Material. The remainder of the ADP moiety was unchanged. Amino acid residues that were missing from the crystal structure (aa 1, 206–208, 501–507, 622–626, and 760–762) were added to the model using the program O (30) to create a continuous chain. All MD simulations used the Amber 8 suite of programs (31) using the Cornell force field (32) with modifications taken from the Generalized Amber Force Field (33). Charges for the nucleotides were derived by first carrying out a single-point energy calculation at the Hartree-Fock level of theory using a 6-31G* basis set to obtain electrostatic charges with Gaussian03 (34). These were then fit to the molecules by using the RESP procedure (35). Hydrogen atoms were added using the LEaP module of Amber. Van der Waals parameters for the Mg^{2+} that cofactors the nucleotide were taken from (36) and adjusted as described in (37). Na^+ ions were added using a Coulombic potential on a grid to insure charge neutrality. The molecule was solvated in a box of TIP3P water molecules (38), with a minimum 10 Å distance from the molecule to the edge of the box. An energy minimization was then done to generate the starting structure for a MD simulation using 1500 steps of the method of steepest descent followed by 1500 steps of conjugate gradient minimization.

The particle mesh Ewald method (39–41) was used for calculating the electrostatic part of the potential energy term for the MD simulation. The time-evolution of the system was followed at constant pressure with gradual heating to 300 K. Temperature was maintained using the Berendsen algorithm (42). Periodic boundary conditions were used. The SHAKE algorithm was used (43) with a 1 fs timestep. Total simulation time was 1000 ps with intermediate steps written to disk every 1 ps for analysis. For in silico mutagenesis studies, the Protein Data Bank structure was modified before the above protocols. Simulation results were visualized using the Chimera molecular graphics suite (44). The final models for each of the 1 ns simulations were compared, as well as the average structures derived from the final 5 ps.

RESULTS

Substitution of the base portion of the nucleotide substrate of myosin alters the resulting muscle fiber mechanics. Our goal is to identify the myosin-substrate base interactions that modulate the contractile properties. Thus we have initially used MD simulations to investigate the interaction of ATP with myosin under simulated physiological conditions in an aqueous environment. With ATP at the nucleotide site, the MD-simulated myosin-nucleotide hydrogen-bonding pattern closely matched that of the original myosin·ADP·BeF_3 crystal structure except that the presence of hydrogen atoms in the MD simulation allowed the hydrogen bond orientations to be explicitly defined (Fig. 1). Both the x-ray structure and the MD simulation show that the primary interaction of the base with the protein is via a closed, connected path of hydrogen bonds from the nucleotide through a triad of amino acids as in Scheme 1

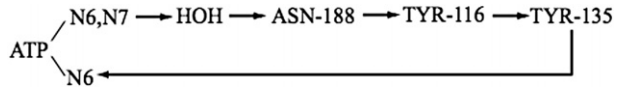

Scheme 1

In addition to forming a hydrogen bond to Tyr-116 and a water-mediated hydrogen bond to ATP, the position of the side chain of Asn-188 is further stabilized by an additional hydrogen bond to the backbone carbonyl of Gly-184 in the P-loop. The hydrogen bond lengths for all of the myosin-adenine ring interactions are virtually ideal, ranging from 1.7 Å to 2.2 Å, suggesting a nucleotide pocket that is highly optimized for binding ATP. There is an additional water-mediated hydrogen bond between the N^1-position of ATP and the backbone amide of Ile-132 in the myosin x-ray structure. This water-mediated interaction was also observed in the MD simulation but appeared highly labile, continuously forming, breaking, and changing partners. Indeed, in the 5 ps final average structure shown in Fig. 1, this water is hydrogen bonded to both the backbone amide of Ile-132 and the backbone carbonyl of Lys-130. With the P-loop, Switch 1 and Switch 2, the loop Phe-129–Ile-132 forms the fourth binding loop at the active site. For more memorable notation, we shall refer to the loop Phe-129–Ile-132 as the N4-loop (3). The binding of the triphosphate portion of ATP in the MD simulation also closely matched that of the x-ray structure. We conclude that the MD simulation accurately reproduces the hydrogen-bonding pattern seen in the x-ray structure, although the transient nature of

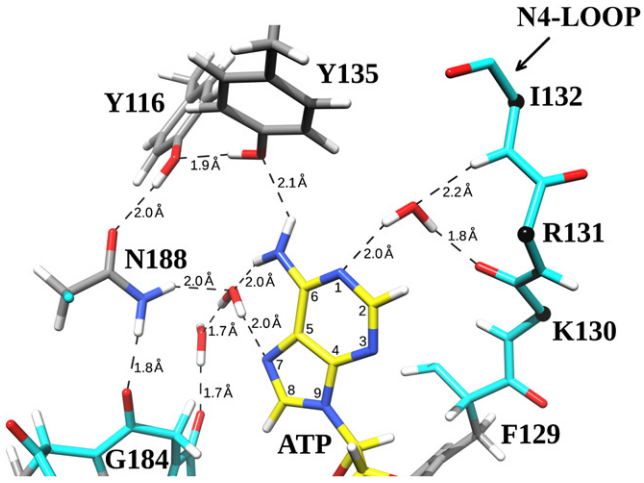

FIGURE 1 MD-simulated interaction of the purine ring of ATP at the nucleotide site of myosin. Interactions are shown with dashed lines with distances in angstroms.

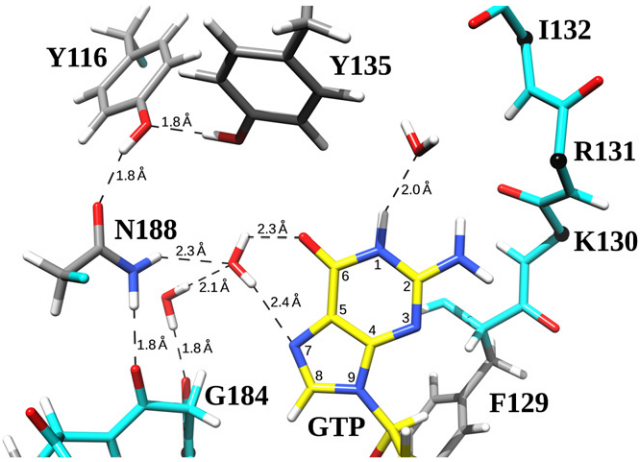

FIGURE 2 Simulated interaction of GTP with myosin.

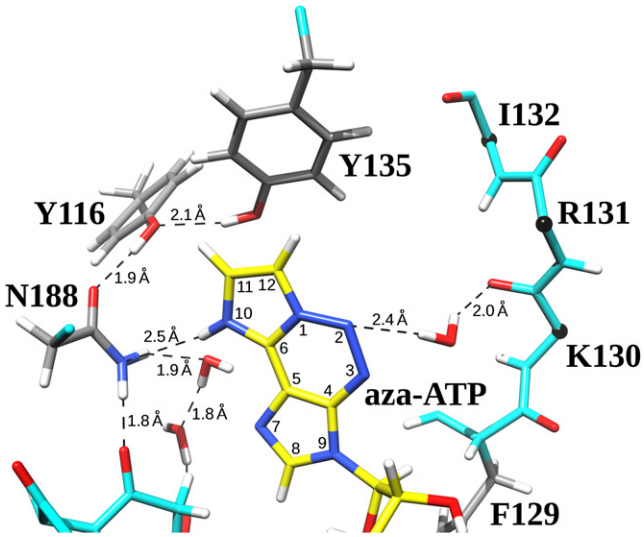

FIGURE 3 Simulated interaction of aza-ATP with myosin.

the hydrogen bond to the N4-loop indicates it is not crucial for function. Our model of ATP-myosin can thus serve as the reference point for comparing the interactions of myosin with other nucleotides.

Firstly, we consider purine-based nucleotides. Fig. 2 shows the interaction of GTP with myosin predicted by the MD simulations. An overlay of the myosin·GTP MD simulation structure and the myosin·ATP MD structure via a least-squares distance minimization on the P-loops places the GTP 6-position carbonyl oxygen only 0.9 Å from the 6-position amine nitrogen of ATP. This close proximity allows the water-mediated hydrogen bond to the side-chain amide of Asn-188 to be maintained. However, due to the required reorientation of the bridging water necessary for hydrogen bonding to the 6-position carbonyl of GTP, the water-mediated hydrogen bonds are slightly longer than was the case for ATP. The side chain of Asn-188 continues to be further stabilized by an additional hydrogen bond to the backbone carbonyl of Gly-184. The triad hydrogen-bonding pattern (Asn-188 ↔ Tyr-116 ↔ Tyr-135) is likewise maintained. No hydrogen bonding was observed with the N4-loop.

The most significant difference between the ATP and GTP coordination is that there cannot be a hydrogen bond between the 6-position carbonyl of GTP and the hydroxyl of Tyr-135. Several alternative possibilities were investigated. The hydroxyl of Tyr-135 was manually rotated, breaking the hydrogen bond between the hydroxyl hydrogen of Tyr-135 and hydroxyl Oγ of Tyr-116 while forming a 2.4 Å hydrogen bond between the hydroxyl hydrogen of Tyr-135 and the GTP 6-position carbonyl oxygen. The hydroxyl of Tyr-116 could likewise then be rotated to re-establish a hydrogen bond with Tyr-135. These structures were stable during the dynamical portion of the MD simulation (data not shown). Thus although a number of perturbations were possible with GTP at the active site, there was no way to maintain the complete circular pattern of interactions with Tyr-135, Tyr-116, Asn-188, and nucleotide that was inferred to be crucial from the ATP x-ray structure and the MD simulation. Simulations with ITP gave the same result (data not shown).

1-N^6-etheno-2-aza-ATP (aza-ATP) is a fluorescent ATP analog containing an etheno-ring bridging the C^6- and N^1-positions of the adenine ring (Fig. 3) (45). aza-ATP is hydrolyzed by myosin, but its ability to generate force in mechanical assays is severely reduced relative to ATP (Table 1). Fig. 3 shows the results of the simulation of aza-ATP docked at the myosin nucleotide site. The simulations indicate that this analog is unable to form a hydrogen bond with Tyr-135 because the N^1- and the C^6-positions are both blocked by the extra etheno-ring. The water molecule that normally mediates the connection between N^7 and Asn-188 moved to a distance of 2.8 Å from N^7, although it remained hydrogen bonded to Asn-188. The water-mediated interaction with the backbone carbonyl of N4-loop Lys-130 was via the N^2-position of aza-ATP, rather than a water-mediated interaction between the N^1-position and the backbone amide of Ile-132 as in ATP.

The base portion of aza-ATP remained tightly bound in the nucleotide pocket, but in a slightly altered position relative to ATP. A superposition of the final 5 ps average structures from the ATP and aza-ATP showed that the C^6-position of aza-ATP was displaced by 2.1 Å further into the nucleotide pocket toward Asn-188. The distance from the aza-ATP N^{10} to the Cα-backbone atom of Asn-188 is 4.1 Å. For ATP, the comparable distance from the 6-position amino nitrogen is 6.1 Å. The displacement is due to favorable hydrophobic and van der Waals interactions between the etheno-ring of aza-ATP and the aromatic rings in the side chains of Tyr-135, and to a lesser extent, Tyr-116. The etheno-ring comes within 3.5 Å of the Tyr-135 aromatic ring in a nearly parallel alignment, suggesting favorable stacking interactions. There also appears to be a weak, polar interaction between the N^{10}-hydrogen of the etheno-ring of aza-ATP

TABLE 1 Mechanical parameters for modeled nucleotides given relative to the ATP value

Substrate	V_{max} of shortening	Isometric tension
ATP	1	1
CTP	0.70 (19)	0.80 (19)
	1.01 (22)	0.86 (22)
UTP	0.76 (22)	0.47 (22)
aza-ATP	0.24 (19)	0.25 (19)
ITP	0.07 (22)	0.11 (22)
GTP	0.05 (19)	0.10 (19)
	0.04 (22)	0.17 (22)

Data from skinned rabbit psoas fibers. Values are normalized with respect to ATP.

and the side chain amide nitrogen of Asn-188. The spatial relationship between ATP and aza-ATP in the superposition of the two structures is shown in more detail in Fig. S2.

With pyrimidines, there are two possible orientations of the ring. To fix notation, we will refer to the orientation of the ring with the 2- and 3-positions facing into the nucleotide pocket as the A-orientation and with the 4- and 5-positions facing into the nucleotide pocket as the B-orientation. When ATP was replaced by CTP at the nucleotide site in the A-orientation, the MD-simulated hydrogen-bonding pattern between the base and the interior of the nucleotide site was virtually identical to that obtained with ATP (Fig. 4 *a*). Overlaying the simulated ATP and CTP structures shows the C^4-amide nitrogen of CTP to be only 0.9 Å away from the C^6-amide nitrogen of ATP. This close proximity allows there to be a 2.6 Å hydrogen bond between one of the hydrogen atoms in the ring C^4-amide and the hydroxyl hydrogen of Tyr-135. Likewise, there is a water-mediated hydrogen bond between the N^3 ring position and the terminal amide of Asn-188. The side chain of Asn-188 is further stabilized by a hydrogen bond to the backbone carbonyl of Gly-184. The triad of interactions between Asn-188, Tyr-116, and Tyr-135 is likewise maintained. Thus the only small difference between the ATP and CTP interactions with myosin is that the water-mediated hydrogen bond between the base N^7-position and the backbone carbonyl of Ile-132 with bound ATP is now replaced by a water-mediated hydrogen bond between the other ring C^4-amide hydrogen and the backbone carbonyl of Lys-130. The surprising observation is that in the B-orientation (Fig. 4 *b*), a similar coordination is possible. There is again a direct hydrogen bond between the ring C^4-amide and the hydroxyl hydrogen of Tyr-135. There is a water-mediated hydrogen bond between the ring C^4-amide and the terminal amide of Asn-188. The triad of amino acid interactions is likewise maintained. There is a water-mediated hydrogen bond from the N^3-position to the backbone carbonyl of Lys-130. Thus although different elements of the pyrimidine ring are involved, the coordination to the protein is remarkably similar in both the A- and B-orientations of the ring.

Fig. 5, *a* and *b*, give the modeled interaction of UTP in the two orientations of the pyrimidine ring. The hydrogen-bonding interaction of Asn-188, Tyr-116, and Tyr-135 are maintained as in the case of ATP. In the A-orientation (Fig. 5 *a*) there is a single water bridge to Tyr-135. The hydrogen-bonding pattern to Asn-188 is not as tightly coupled as with ATP. There is now a two-water hydrogen-bond bridge to Asn-188. With UTP in the B-orientation (Fig. 5 *b*), the hydrogen-bonding bridges are similar. Most interestingly, in both cases, the waters in the constellations between the nucleotide and the two amino acids also interact with each other. This implies that in the face of additional conformational changes at the nucleotide site, a more favorable hydrogen-bonding pattern to one of the amino acids, Tyr-135 or Asn-188, can only be done at the expense of the other. Both orientations show hydrogen bonding to the N4-loop.

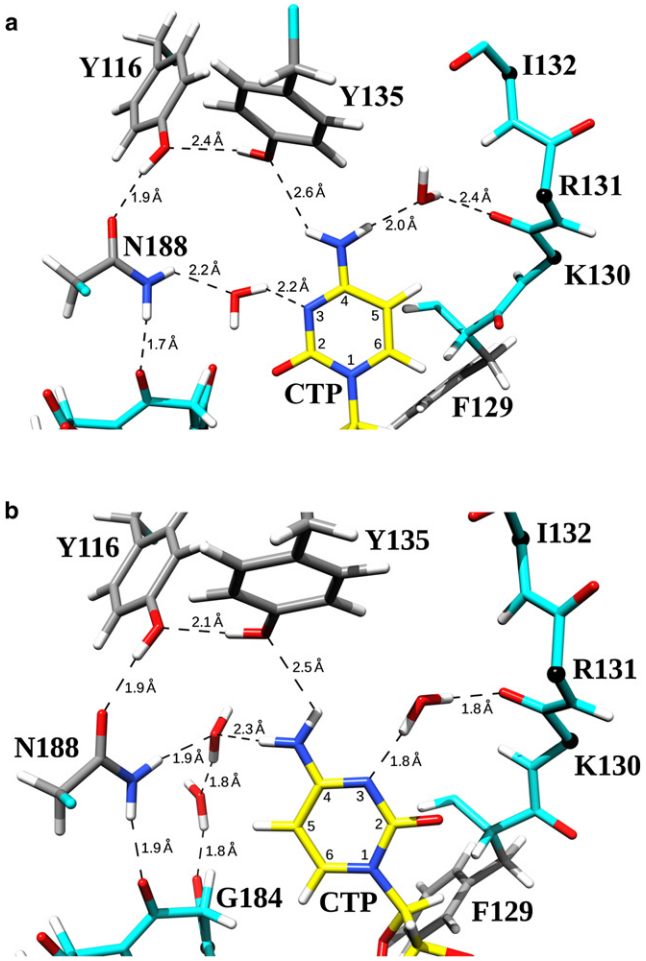

FIGURE 4 Simulated interaction of CTP with myosin in the (*a*) A-orientation and (*b*) B-orientation.

DISCUSSION

We have used MD simulations to compare the interaction of ATP and other nucleotides with the myosin active site. Table 1 compares the mechanical properties of ATP with the nucleotides we have simulated. In terms of efficacy as mechanical

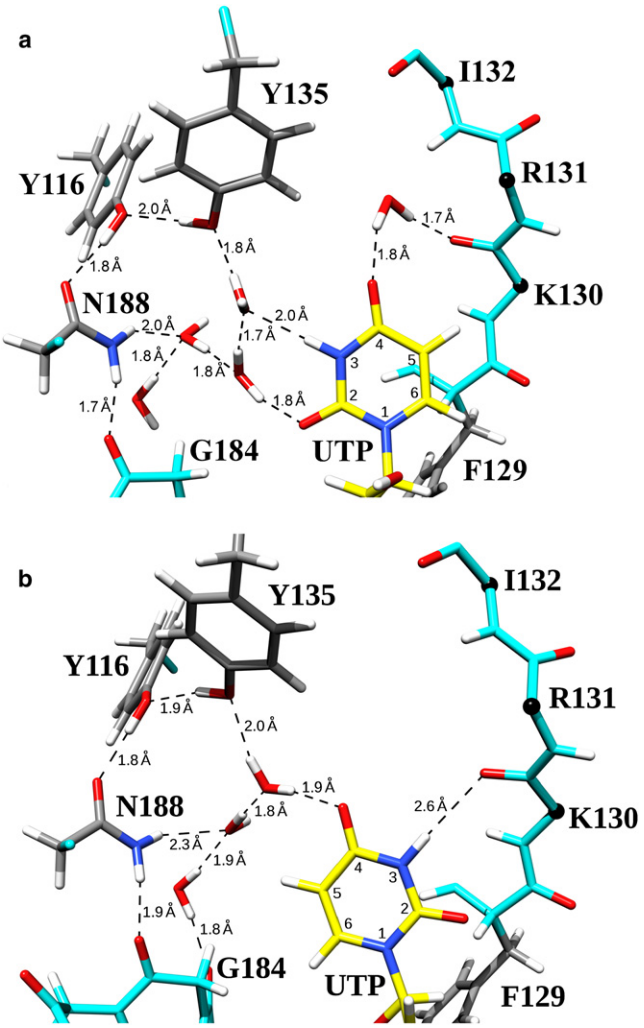

FIGURE 5 Simulated interaction of UTP with myosin in the (*a*) A-orientation and (*b*) B-orientation.

substrates, the analogs can be ordered ATP > CTP > UTP > aza-ATP > ITP > GTP, with the rightmost three being particularly poor substrates. ATP forms the closed-loop hydrogen-bonding pattern in the nucleotide pocket given by Scheme 1. As discussed below, the simulations argue that the efficacy of the nucleotide analogs is graded by their ability to duplicate the hydrogen-bonding pattern in Scheme 1.

The purine, GTP, is the least effective of the simulated nucleotides. There have been suggestions previously that it is the modification of the 6-position of the purine ring from an amine to a carbonyl that modulates function (19,22,25). The simulations suggest that, although this is correct, the reason is more complicated. As seen in Fig. 2, with the orientation of the three key amino acids (Asn-188, Tyr-116, and Tyr-135) as in the ATP MD simulation and x-ray structure, the 6-position carbonyl of GTP cannot hydrogen bond to the hydroxyl of the closest amino acid, Tyr-135. However, the simulations showed that a rotation of the side chain of Tyr-135 resulted in a stable conformation on MD simulation timescales of the nucleotide pocket with the 6-position carbonyl forming a 2.4 Å hydrogen bond with the hydroxyl of Tyr-135. A hydrogen bond to the same hydroxyl is seen in the ATP x-ray structure and the MD simulation. Thus the MD simulation suggests that it is not the inability to form a single hydrogen bond similar to that seen with ATP that is the culprit, but that in forming this hydrogen bond, it becomes impossible to maintain the coordination of the triad seen in Scheme 1. The same was found to hold for ITP.

Although aza-ATP is a more efficacious substrate than GTP or ITP, it remains an extremely poor substrate for the actomyosin system. However, the MD simulations imply that aza-ATP is better able to maintain at least an approximation to the coordination seen in Scheme 1 (Fig. 3). The hydrogen-bonding pattern of Scheme 1 is modified in two places. There is only a weak ionic interaction between the nucleotide ring and Asn-188. There is no hydrogen bond between the nucleotide and Tyr-135. However, there is a weak but clear hydrophobic interaction between the etheno-ring of aza-ATP and the phenyl ring of Tyr-135. Thus although aza-ATP remains a very poor substrate for myosin, the modeling provides a rationale for it being a slightly better substrate than either GTP or ITP.

The pyrimidines can assume two orientations in the active site. The surprising observation was that in either orientation, both CTP and UTP were able to retain the hydrogen-bonding pattern seen with ATP. For CTP the similarity to the ATP pattern was particularly striking. Superposition of the CTP structure with the ATP structure from MD simulation (and the x-ray structure) showed a close correlation between the location of the ATP and CTP ring amines. This allowed CTP to reproduce the ATP interaction pattern, but with the hydrogen bonding distances slightly lengthened. With UTP, there were additional waters added into a water constellation between the pyrimidine ring and the triad of amino acids. Consistent with the ability to mimic the ATP coordination, CTP is an extremely effective substrate. UTP with the extra water molecules forms a less tight coupling to the interior of the nucleotide site. It is an effective substrate, but now not surprisingly, a less effective mechanical substrate than CTP.

The question remains regarding any potential preferred orientation at the active site. The simulations suggest that either orientation would function approximately equally, irrespective of the relative binding affinities of the two orientations. The only independent evidence for orientation comes from photoaffinity labeling experiments with UTP at the active site of smooth muscle myosin subfragment 1 identifying Glu-185 at the active site (homologous to Glu-187 of *Dictyostelium* myosin) (46–48). The C^5-C^6 double bond is thought to be the photoreactive center of the pyrimidine ring (48–50), suggesting binding in the B-orientation. The ~60% photo-incorporation of the vanadate-trapped nucleotide (48) could be taken to suggest a slight preference for the B-orientation over the A-orientation, although photo-incorporation has not been shown to be a quantitative assay.

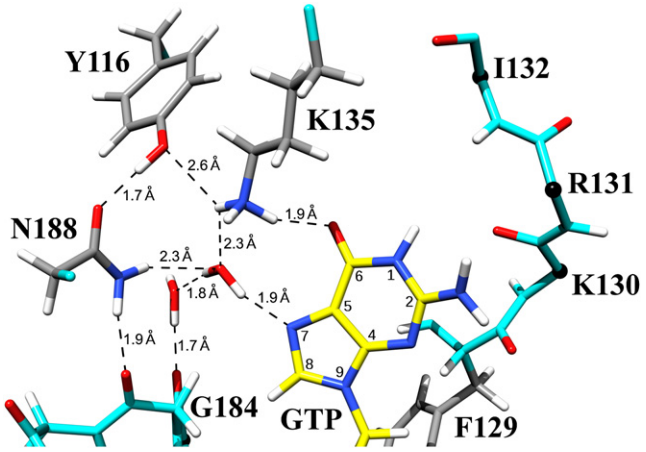

FIGURE 6 Simulated interaction of GTP with a myosin having the mutation Y135K.

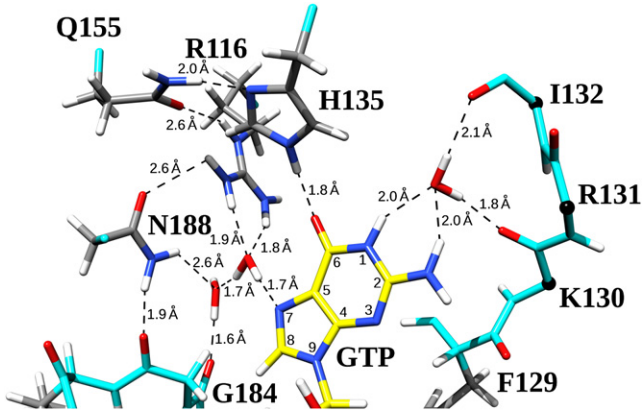

FIGURE 7 Simulated interaction of GTP with a myosin having the mutation Y135H, Y116R, I155Q.

Can one enhance the function of myosin as a GTPase?

The important observation from the MD simulations is that the ability of nucleotides to function as mechanical substrates correlates well with the degree to which they mimic the Scheme 1 coordination of the nucleotide ring. As an additional test of the modeling, the question then becomes whether one can use the analyses to suggest modifications to the nucleotide pocket that can upregulate poor substrates while simultaneously downregulating ATP. GTP and ATP have the greatest difference in function. Thus we have concentrated on this nucleotide pair to show that the modeling does have predictive capabilities.

The modeling indicates that a crucial interaction is at the 6-position of the purine ring. The goal becomes to replace the hydroxyl oxygen of Tyr-135 with a positive charge while maintaining the coordination of Scheme 1. Fig. 6 shows the hydrogen-bonding pattern for the mutation Y135K with GTP at the active site. With the lysine being fully ionized, the interactions of Scheme 1 are maintained. However, both Lys-135 and the N^7-position of the GTP base now interact. Our observations with UTP suggest this type of multiple-interaction is an additional downregulating factor for this mutation. Nonetheless, all other things being equal, Y135K *Dictyostelium* myosin would still be expected to be a better GTPase and worse ATPase than wild-type myosin. Other mutations were also examined including Y135/E, N, Q, R, and T. None seemed to enhance GTP functionality in terms of the coordination identified in Scheme 1. An alternative mutation involves more side chains to offer a potentially more flexible interaction. Fig. 7 gives the MD-simulated interaction for the triple mutation Y135H, Y116R and I155Q. The mutation again allows a hydrogen-bonding pattern to be established that is similar to Scheme 1, but with one additional intervening amino acid. Coordination to the N4-loop is likewise maintained. ATP has been docked at the active site of both mutants and as expected, the hydrogen-bonding pattern of Scheme 1 is disrupted (data not shown). The regulation of myosin function is a complex process, most certainly involving multiple intraprotein interactions and multiple interactions with actin. Most certainly, the interaction of the nucleotide with myosin is not the only determinant of function. However, all other things being equal, the two mutants would be predicted to show diminished function as ATPases and enhanced function as GTPases.

As noted, others (22,25) and we (19) have previously implicated the interaction between the 6-position of the purine base and Tyr-135 as the functionally important interaction. The simulations suggest a more complicated interaction pattern. However, one additional mutation of the active site is important to point out with regard to these two suggestions on the crucial interactions. Fig. 8 shows the MD-simulated interaction of GTP with *Dictyostelium* myosin for the mutation Y135H. The mutation maintains 2.0 Å hydrogen bond between the C^6-carbonyl of GTP and the ε^2-position of the histidine ring. The simulation shows all other interactions proposed as relevant in Scheme 1 with the exception of the hydrogen bond between Y135H and Tyr-116. If it were solely the C^6-Tyr-135 interaction that is crucial, Y135H would be expected to be a functional GTPase. The Scheme 1 interactions would predict that it would not be an effective GTPase or ATPase. We additionally did simulations of the individual mutations Y135F and Y116F. Both disrupted the interactions between the nucleotide and the triad as would be expected from the inability of the phenyl ring to form hydrogen bonds between amino acids 116 and 135 as well as with the 6-position on the nucleotide base.

Are other myosin-substrate interactions involved?

The x-ray structures identify several other potential modulating interactions. The adenine ring sits in a slot formed by a salt-bridge between Arg-131 and Glu-187. In the simulations, the salt-bridge is maintained for ATP, GTP, ITP, and

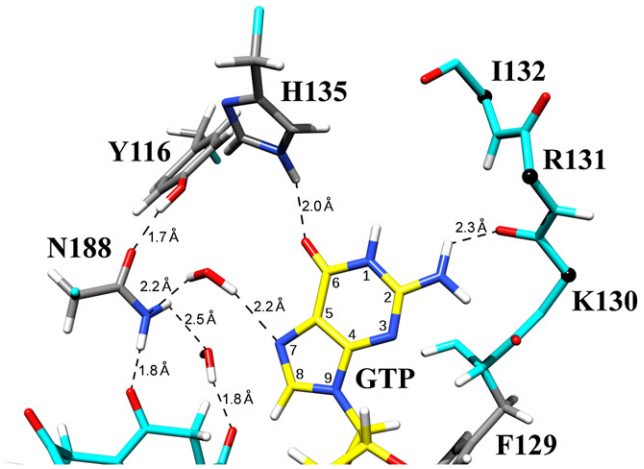

FIGURE 8 Simulated interaction of GTP with myosin having the mutation Y135H.

CTP, whereas it is broken for the others, suggesting that maintenance of the salt-bridge is not an additional modulating factor. X-ray structures further support this conclusion. The salt-bridge is missing in the ADP·VO_4 structure from the Rayment laboratory (PBD ID 1VOM). The x-ray structures also identify an interaction between the ribose ring oxygen and conserved Asn-127. This interaction is present in all simulated structures.

Alternatively, the differing nucleotide activities could result from the triphosphate portions of the nucleotide differing in their interaction with myosin. However, comparison of the simulated ATP and GTP structures with the *Dictyostelium* myosin·ADP·BeF_3 crystal structure showed an identical binding arrangement for the triphosphate portion of the nucleotide. In all three structures, the Mg^{2+} ion was coordinated by the β- and γ-phosphates, two water molecules, and the side chain hydroxyls of Thr-186 and Ser-237. Also in all three structures, the triphosphate moiety formed direct hydrogen bonds with the side chains of Ser-181, Lys-185, Asn-233, and Ser-236. Direct hydrogen bonds were also present between the triphosphate and main chain amide hydrogens of Gly-182, Gly-184, Lys-185, Thr-186, and Glu-187. The only observed difference among the three structures was the presence of an extra water molecule in the simulated structures that was hydrogen bonded to the γ-phosphate and to the side chain hydroxyl of Ser-456. This water was not present in the x-ray structure. The position of this water molecule was variable in the simulations and is likely to be too mobile to be observed in the x-ray structure. Additionally, the hydrogen bond lengths between the amino acids and the γ-phosphate oxygens were monitored during the simulations. The mean bond lengths for the ATP and GTP simulations differed by <0.04 Å for all but Asn-233 where the difference was still <0.25 Å. Similar results were obtained when ATP and GTP were docked in the ADP·VO_4 x-ray structure (5). The maximum difference in the mean ATP and GTP hydrogen bond lengths to the

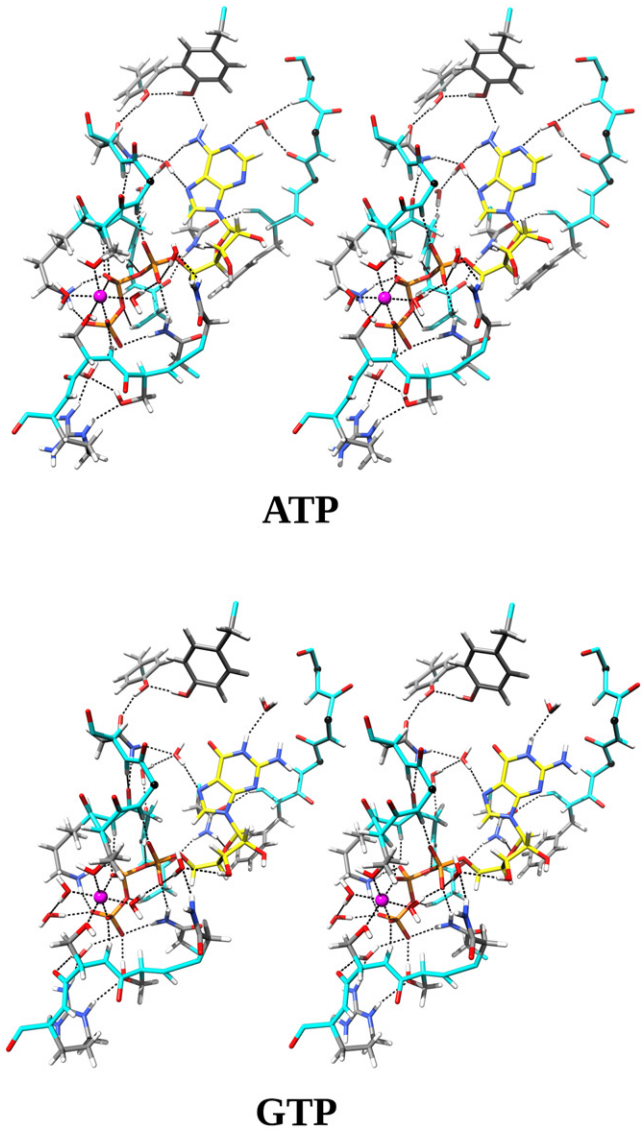

FIGURE 9 Stereo diagram comparing the binding of ATP and GTP to *Dictyostelium* myosin. The multi-coordinated sphere is the Mg^{2+} ion.

γ-phosphate oxygens for these simulations was only 0.07 Å. The similarity is surprising considering the different hydrolysis kinetics for ATP and GTP (18). However, it is important to remember that MD simulations are on the nanosecond timescale. We cannot rule out the possibility of more significant differences on longer timescales, the possibility that very subtle changes in hydrogen bond lengths are critical, or that other crucial x-ray structures defining the myosin-nucleotide interaction remain to be determined. Stereo pair diagrams of the interactions of ATP and GTP with the myosin nucleotide site are shown in Fig. 9.

We have examined the interaction of a series of nucleotides with a cluster of three amino acids at the nucleotide site in *Dictyostelium* myosin II. A relevant question becomes the degree to which these amino acids are conserved across myosin isoforms. Tyr-116 and Tyr-135 are highly, but not

universally conserved. There is more extensive variation at residues homologous to Asn-188 (51,52). This introduces the additional possibility of isoform-specific regulation of myosin function via perturbation of these residues. For example, restricting attention to the more variable Asn-188 residue in *Dictyostelium* myosin II, myosin V has a serine residue at the homologous location (Ser-172, PDB ID 1W7J). Myosin I has an alanine. Both conserve the tyrosine pair. There is no x-ray structure of myosin I at this writing. We did MD simulations of myosin V and of *Dictyostelium* myosin with the mutation N188A. As expected, in the myosin I simulation, there was no hydrogen-bond interaction between Ala-188 and Tyr-116 breaking the chain of interactions in Scheme 1 (data not shown). The myosin V simulation gave a hydrogen-bonding pattern virtually identical to the x-ray structure; again demonstrating that MD simulation accurately reproduces x-ray results. A water molecule inserted itself between Tyr-100 (homologous to Tyr-116) and Ser-172 allowing the Scheme 1 hydrogen-bond interaction among the amino acids and to the 6-position of the base to be maintained (data not shown). With the shorter side chain for the serine, the hydrogen-bonding pattern from the base N^7-position now involved multiple waters and also included the water bridging between Tyr-100 and Ser-172. The simulations with UTP suggest that multiple waters and branched hydrogen-bonding patterns downregulate function. Myosin V and Myosin I both have slower translation velocities and ATPase rates than myosin II. We are again not implying that the amino acids in the nucleotide pocket are the sole regulatory determinant of myosin function. However, they are potentially one of the determinants. In this particular case, all other things being equal, replacing the alanine or serine with an asparagine would be expected to produce a protein more like myosin II in function.

In summary, we have examined the interaction with the nucleotide pocket of *Dictyostelium* myosin II of a series of nucleotides that exhibit varied mechanical efficacy. The efficacy correlates well with the ability of the substrates to duplicate the cyclical coordination of ATP and three amino acids seen in the x-ray structure. The regulation of myosin function is a complex process involving numerous interactions. However, it would seem that a previously unrecognized set of regulatory interactions could function in an isoform-specific manner. The MD simulations find no significant difference between the interactions of the triphosphate moiety with myosin as a function of the base. ATP and GTP differ in efficacy by an order of magnitude. The lack of a difference in coordination is problematic for models that posit that the interaction of the triphosphate moiety with myosin is the sole determinant of function.

SUPPORTING MATERIAL

Two figures are available at http://www.biophysj.org/biophysj/supplemental/S0006-3495(09)01280-6.

This work was supported by National Institutes of Health grants AR053720 (E.P., D.H.) and AR042895 (R.C.). Molecular visualization was done using the facilities of the University of California, San Francisco, Computer Graphics Laboratory supported by National Institutes of Health grant RR001081, T. Ferrin, PI.

REFERENCES

1. Kull, F. J., R. D. Vale, and R. J. Fletterick. 1998. The case for a common ancestor: kinesin and myosin motors and G proteins. *J. Muscle Res. Cell Motil.* 19:877–886.
2. Smith, C. A., and I. Rayment. 1996. Active site comparisons highlight structural similarities between myosin and other P-loop proteins. *Biophys. J.* 70:1590–1602.
3. Vale, R. D. 1996. Switches, latches, and amplifiers: common themes of G proteins and molecular motors. *J. Cell Biol.* 135:291–302.
4. Fisher, A. J., C. A. Smith, J. B. Thoden, R. Smith, K. Sutoh, et al. 1995. X-ray structure of the myosin motor domain of *Dictyostelium discoideum* complexed with MgADP·BeFx and MgADP·AlF4-. *Biochemistry.* 34:8960–8972.
5. Smith, C. A., and I. Rayment. 1996. X-ray structure of the magnesium(II). ADP·vanadate complex of the *Dictyostelium discoideum* myosin motor domain to 1.9 A resolution. *Biochemistry.* 35:5404–5417.
6. Rayment, I., W. R. Rypniewski, K. Schmidt-Base, R. Smith, D. R. Tomchick, et al. 1993. Three-dimensional structure of myosin subfragment-1: a molecular motor. *Science.* 261:50–58.
7. Cooke, R. 1997. Actomyosin interaction in striated muscle. *Physiol. Rev.* 77:671–697.
8. Geeves, M. A., and K. C. Holmes. 1999. Structural mechanism of muscle contraction. *Annu. Rev. Biochem.* 68:687–728.
9. Holmes, K. C. 1997. The swinging lever-arm hypothesis of muscle contraction. *Curr. Biol.* 7:R112–R118.
10. Holmes, K. C., and M. A. Geeves. 2000. The structural basis of muscle contraction. *Philos. Trans. R. Soc. Lond. B Biol. Sci.* 355:419–431.
11. Li, G., and Q. Cui. 2003. Mechanochemical coupling in myosin: a theoretical analysis with molecular dynamics and combined QM/MM reaction path calculations. *J. Phys. Chem. B.* 108:3342–3357.
12. Kawakubo, T., O. Okada, and T. Minami. 2005. Molecular dynamics simulations of evolved collective motions of atoms in the myosin motor domain upon perturbation of the ATPase pocket. *Biophys. Chem.* 115:77–85.
13. Fischer, S., B. Windshugel, D. Horak, K. C. Holmes, and J. C. Smith. 2005. Structural mechanism of the recovery stroke in the myosin molecular motor. *Proc. Natl. Acad. Sci. USA.* 102:6873–6878.
14. Yu, H., L. Ma, Y. Yang, and Q. Cui. 2007. Mechanochemical coupling in the myosin motor domain. II. Analysis of critical residues. *PLOS Comput. Biol.* 3:e23.
15. Woo, H. J. 2007. Exploration of the conformational space of myosin recovery stroke via molecular dynamics. *Biophys. Chem.* 125:127–137.
16. Koppole, S., J. C. Smith, and S. Fischer. 2006. Simulations of the myosin II motor reveal a nucleotide-state sensing element that controls the recovery stroke. *J. Mol. Biol.* 361:604–616.
17. Shibata-Sekiya, K. 1973. ATP analogues. *In* Muscle Proteins, Muscle Contraction and Cation Transport. Y. Tonomura, editor. University Park Press, Baltimore, MD. 259–271.
18. White, H. D., B. Belknap, and W. Jiang. 1993. Kinetics of binding and hydrolysis of a series of nucleoside triphosphates by actomyosin-S1. Relationship between solution rate constants and properties of muscle fibers. *J. Biol. Chem.* 268:10039–10045.
19. Pate, E., K. Franks-Skiba, H. White, and R. Cooke. 1993. The use of differing nucleotides to investigate cross-bridge kinetics. *J. Biol. Chem.* 268:10046–10053.
20. Cremo, C. R., J. M. Neuron, and R. G. Yount. 1990. Interaction of myosin subfragment 1 with fluorescent ribose-modified nucleotides. A

comparison of vanadate trapping and SH1–SH2 cross-linking. *Biochemistry*. 29:3309–3319.

21. Regnier, M., and E. Homsher. 1998. The effect of ATP analogs on post-hydrolytic and force development steps in skinned skeletal muscle fibers. *Biophys. J.* 74:3059–3071.
22. Regnier, M., D. M. Lee, and E. Homsher. 1998. ATP analogs and muscle contraction: mechanics and kinetics of nucleoside triphosphate binding and hydrolysis. *Biophys. J.* 74:3044–3058.
23. Seow, C. Y., H. D. White, and L. E. Ford. 2001. Effects of substituting uridine triphosphate for ATP on the crossbridge cycle of rabbit muscle. *J. Physiol.* 537:907–921.
24. Belknap, B., X.-Q. Wang, and H. White. 1994. Rate and equilibrium constants of the hydrolysis of a series of nucleoside triphosphates by myosin-S1. *Biophys. J.* 66:A79.
25. White, H. D., B. Belknap, and M. R. Webb. 1997. Kinetics of nucleoside triphosphate cleavage and phosphate release steps by associated rabbit skeletal actomyosin, measured using a novel fluorescent probe for phosphate. *Biochemistry*. 36:11828–11836.
26. Pate, E., K. L. Nakamaye, K. Franks-Skiba, R. G. Yount, and R. Cooke. 1991. Mechanics of glycerinated muscle fibers using nonnucleoside triphosphate substrates. *Biophys. J.* 59:598–605.
27. Wang, D., E. Pate, R. Cooke, and R. Yount. 1993. Synthesis of non-nucleotide ATP analogues and characterization of their chemomechanical interaction with muscle fibers. *J. Muscle Res. Cell Motil.* 14:484–497.
28. Nakamaye, K. L., J. A. Wells, R. L. Bridenbaugh, Y. Okamoto, and R. G. Yount. 1985. 2-[(4-Azido-2-nitrophenyl)amino]ethyl triphosphate, a novel chromophoric and photoaffinity analogue of ATP. Synthesis, characterization, and interaction with myosin subfragment 1. *Biochemistry*. 24:5226–5235.
29. Gulick, A. M., C. B. Bauer, J. B. Thoden, E. Pate, R. G. Yount, et al. 2000. X-ray structures of the *Dictyostelium discoideum* myosin motor domain with six non-nucleotide analogs. *J. Biol. Chem.* 275:398–408.
30. Jones, T. A. 1978. A graphics model building and refinement system for macromolecules. *J. Appl. Cryst.* 11:268–272.
31. Case, D. A., T. A. Darden, T. E. Cheatham, 3rd, C. L. Simmerling, R. E. Wang, et al. 2004. AMBER 8. University of California, San Francisco, CA.
32. Cornell, W. D., P. Cieplak, C. I. Bayly, I. R. Gould, K. M. Merz, et al. 1995. A second generation force field for the simulation of proteins. *J. Am. Chem. Soc.* 117:5179–5197.
33. Wang, J., R. M. Wolf, J. W. Caldwell, P. A. Kollman, and D. A. Case. 2004. Development and testing of a general amber force field. *J. Comput. Chem.* 25:1157–1174.
34. Frisch, M. J., G. W. Trucks, H. B. Schlegel, G. E. Scuseria, M. A. Robb, et al. 2004. Gaussian03. Gaussian, Wallingford, CT.
35. Bayly, C. I., W. D. Ciepak, W. D. Cornell, and P. A. Kollman. 1993. A well-behaved electrostatic potential based method using charge restraints for deriving atomic charges: the RESP model. *J. Phys. Chem.* 97:10269–10280.
36. Aqvist, J. 1992. Modelling of ion-ligand interactions in solutions and biomoleculaes. *J. Mol. Struct. (Theochem.).* 256:135–152.
37. Minehardt, T. J., R. Cooke, E. Pate, and P. A. Kollman. 2001. Molecular dynamics study of the energetic, mechanistic, and structural implications of a closed phosphate tube in ncd. *Biophys. J.* 80:1151–1168.
38. Jorgensen, W. L., J. Chandrasekar, J. D. Madura, R. W. Impey, and M. L. Klein. 1983. Comparison of simple potential functions for simulating liquid water. *J. Comput. Phys.* 79:926–935.
39. Darden, T., and D. York. 1993. Particle mesh Ewald—an Nlog(N) method for Ewald sums in large systems. *J. Chem. Phys.* 98:10089–10092.
40. Essman, U., M. Preera, T. Berkowitz, H. Darden, and G. Pedersen. 1995. A smooth particle mesh Ewald method. *J. Chem. Phys.* 103:8577–8593.
41. Hawkins, G. D., C. J. Cramer, and D. G. Truhlar. 1996. Parameterized models of aqueous free energies of solvation based on pairwise descreening of solute atomic charges from a dielectric medium. *J. Chem. Phys.* 100:19824–19839.
42. Berendsen, H. J. C., J. P. M. Postma, W. F. v. Gunsteren, A. DiNola, and J. R. Ghaak. 1984. Molecular dynamics with coupling to an external bath. *J. Chem. Phys.* 113:3684–3690.
43. Ryckaert, A. J., G. Ciccotti, and H. J. C. Berendsen. 1977. Numerical integration of the cartesian equations of motion of a system with constraints: molecular dynamics of n-alkanes. *J. Comput. Phys.* 23:327–341.
44. Pettersen, E. F., T. D. Goddard, C. C. Huang, G. S. Couch, D. M. Greenblatt, et al. 2004. UCSF Chimera—a visualization system for exploratory research and analysis. *J. Comput. Chem.* 25:1605–1612.
45. Secrist, 3rd, J. A., J. R. Barrio, and N. J. Leonard. 1972. A fluorescent modification of adenosine triphosphate with activity in enzyme systems: 1,N 6 -ethenoadenosine triphosphate. *Science*. 175:646–647.
46. Maruta, H., and E. D. Korn. 1981. Direct photoaffinity labeling by nucleotides of the apparent catalytic site on the heavy chains of smooth muscle and Acanthamoeba myosins. *J. Biol. Chem.* 256:499–502.
47. Atkinson, M. A., E. A. Robinson, E. Appella, and E. D. Korn. 1986. Amino acid sequence of the active site of Acanthamoeba myosin II. *J. Biol. Chem.* 261:1844–1848.
48. Garabedian, T. E., and R. G. Yount. 1990. Direct photoaffinity labeling of gizzard myosin with [3H]uridine diphosphate places Glu^{185} of the heavy chain at the active site. *J. Biol. Chem.* 265:22547–22553.
49. Smith, K. C. 1969. Photochemical addition of amino acids to ^{14}C-uracil. *Biochem. Biophys. Res. Commun.* 34:354–357.
50. Wang, S.-Y. 1976. Pyrimidine bimolecular photoproducts. *In* Photochemistry and Photobiology of Nucleic Acids. S.-Y. Wang, editor. Academic Press, New York, NY. 295–356.
51. Cope, M. J., J. Whisstock, I. Rayment, and J. Kendrick-Jones. 1996. Conservation within the myosin motor domain: implications for structure and function. *Structure*. 4:969–987.
52. Hodge, T., and J. Cope. 2000. Myosin motor domain sequence color alignment. http://www.mrc-lmb.cam.ac.uk/myosin/trees/colour.html.